GEOLOGIC MAP OF THE BISON MOUNTAIN 7.5′ QUADRANGLE, POWELL AND JEFFERSON COUNTIES, MONTANA

Pamphlet to Accompany Map

Kaleb C. Scarberry, Ethan L. Coppage, and Alan R. English

Montana Bureau of Mines and Geology

Geologic Map 71

Cover image: View from Tertiary rhyolite outcrops south into Larabee Gulch.

GEOLOGIC MAP OF THE BISON MOUNTAIN 7.5′ QUADRANGLE, POWELL AND JEFFERSON COUNTIES, MONTANA

Pamphlet to Accompany Map

December 2018

Kaleb C. Scarberry,

Ethan L. Coppage,

and Alan R. English

Montana Bureau of Mines and Geology

Geologic Map 71

Partial support has been provided by the STATEMAP component of the National Cooperative Geologic Mapping Program of the U.S. Geological Survey under contract G16AC00196

TABLE OF CONTENTS

FIGURES

TABLES

GEOLOGIC SUMMARY

Paleozoic–Cretaceous sedimentation occurred in a shallow, marine to non-marine environment. Shortening, intrusion of the Boulder Batholith, and coeval eruption of the Elkhorn Mountains Volcanic field (EMVF) thickened the sedimentary thrust wedge by around 16–17 km between about 85 and 74 Ma (Lageson and others, 2001; ages of EMVF from Olson and others, 2016). The Bison Mountain 7.5′ quadrangle lies within the Helena Salient (fig. 1), formed during orogenic collapse of the Montana fold-thrust belt beginning at around 100 Ma (Hyndman and others, 1975; Sears, 2016).

Late Cretaceous Cordilleran arc magmatism (e.g., Rutland and others, 1989) produced the EMVF between about 85 and 77 Ma (Olson and others, 2016; Korzeb and others, 2018). Precious and base metal hydrothermal mineral deposits followed emplacement of granite (Kg) into its volcanic roof, the EMVF, at approximately 74 Ma (ages summarized in Olson and others, 2016). The EMVF is around 1.5 km (0.9 mi) thick in the Bison Mountain 7.5′ quadrangle, where it consists of basaltic andesite–andesite lavas (Keml), diorite intrusions (Kdi), breccia, debris flows and tuff (Kat), and intercalated andesite–dacite lavas, domes, and volcanogenic sediments (Keld). These rocks are overlain primarily by rhyolite ignimbrite (Kemr) (table 1, fig. 2C). High-angle normal faulting contributed to exhumation of the Late Cretaceous magma system (Ruppel, 1963; Wallace and others, 1990; Schmidt and others, 1994).

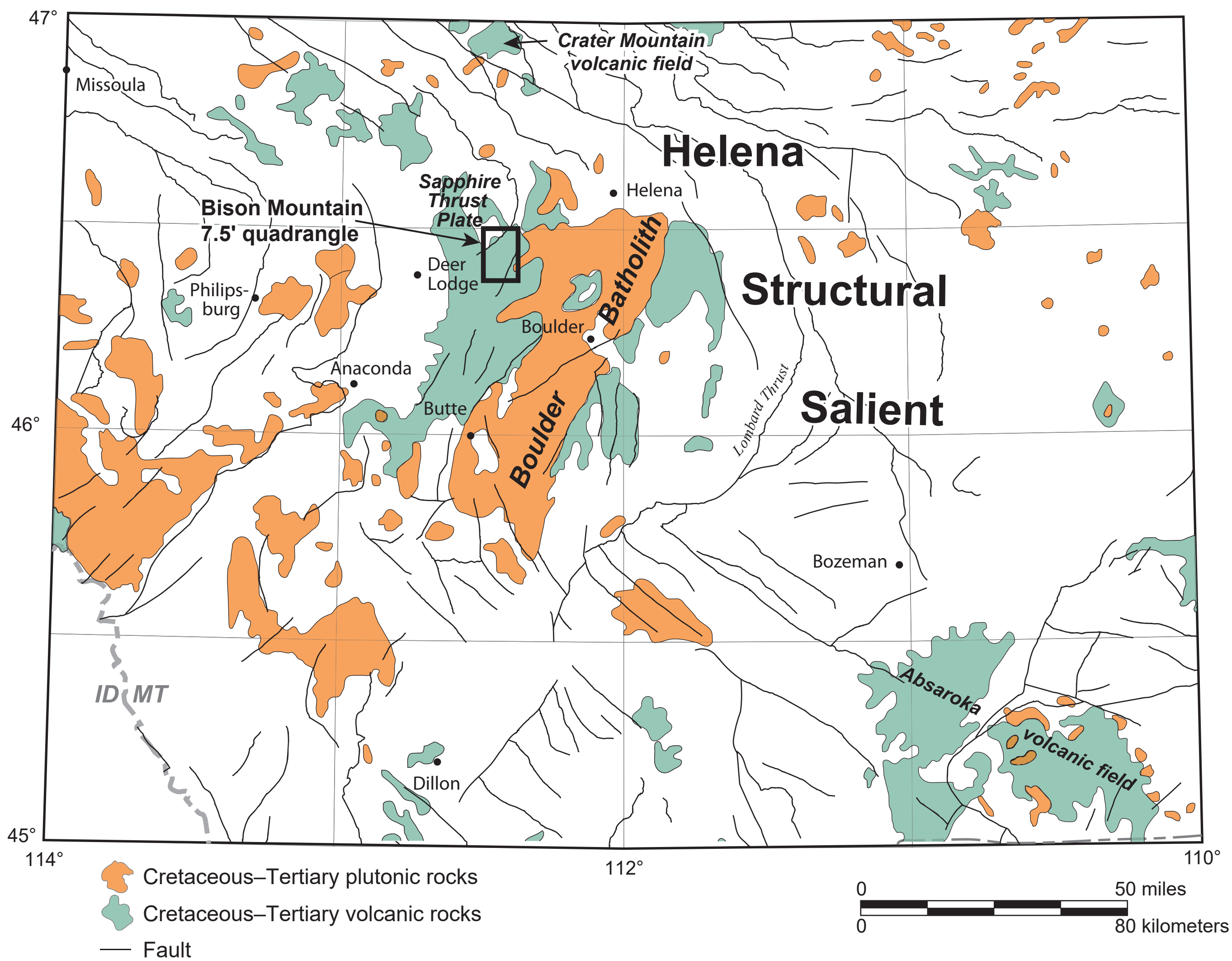

Figure 1. Location of the Bison Mountain 7.5′ quadrangle in the Helena structural salient and igneous geology of the Boulder Batholith and surrounding region. Geology modified from Vuke and others (2007).

Table 1. Major oxide and trace element geochemical data. Major oxides normalized to 100% anhydrous.

Sample ID	KCS-16-17	KCS-16-34	KCS-16-45	KCS-16-33	KCS-16-46	KCS-16-12	8-9-7B	KCS-16-32	KCS-16-40	KCS-16-41	KCS-16-18a
Map unit	**Keml**	**Keml**	**Keml**	**Keml**	**Kdi**	**Kat**	**Kat (clast)**	**Kat**	**Kat**	**Kat**	**Keld**
Lat	**46.45725**	**46.43372**	**46.44277**	**46.43910**	**46.43984**	**46.47642**	**46.42772**	**46.42897**	**46.43941**	**46.44447**	**46.44829**
Long	**-112.43176**	**-112.45035**	**-112.43471**	**-112.44910**	**-112.44764**	**-112.41323**	**-112.45625**	**-112.43407**	**-112.44239**	**-112.44360**	**-112.43840**
XRF (wt. %)											
SiO_2	53.75	55.13	55.34	58.99	54.01	54.37	57.78	61.76	62.03	62.15	62.44
TiO_2	0.90	0.95	0.92	1.01	0.78	1.06	0.95	0.80	0.76	0.75	0.75
Al_2O_3	15.11	14.75	13.56	15.91	17.56	18.05	15.67	17.38	18.11	18.13	17.91
*FeO	8.25	9.03	8.98	8.15	8.52	9.32	5.64	5.54	4.83	4.63	4.69
MnO	0.14	0.18	0.16	0.14	0.11	0.12	0.08	0.10	0.08	0.09	0.09
MgO	5.09	7.27	7.34	3.78	5.11	3.88	3.01	2.39	1.70	1.86	1.84
CaO	10.16	5.54	8.33	5.30	8.06	6.67	6.78	5.01	5.72	6.06	5.62
Na_2O	3.20	3.87	2.55	2.70	2.81	3.97	3.52	3.46	3.28	2.86	3.14
K_2O	2.97	2.85	2.47	3.67	2.69	2.11	5.86	3.32	3.30	3.27	3.31
P_2O_5	0.44	0.45	0.36	0.36	0.37	0.47	0.71	0.24	0.20	0.20	0.20
LOI	3.39	2.63	3.36	6.12	3.23	1.72	5.34	1.96	1.20	1.50	1.57
a.t.	95.69	96.06	96.03	93.37	96.06	97.13	93.86	97.43	98.13	97.59	97.96
Trace elements (ppm) (XRF)											
Ni	88	98	43	14	31	24	18	9	81	10	7
Cr	199	232	318	62	88	39	13	20	156	20	16
Sc	20	20	28	20	21	19	8	14	10	12	12
V	217	177	217	172	199	244	128	116	50	91	92
Ba	753	879	833	1217	985	702	2135	1072	935	1067	1109
Rb	59	68	56	86	58	62	92	90	79	79	83
Sr	947	465	772	553	838	1095	683	716	549	792	786
Zr	156	158	177	255	134	172	196	231	127	252	256
Y	18	22	31	30	19	22	20	23	11	24	24
Nb	9	9	9	12	9	9	12	11	8	11	12
Ga	19	17	16	18	18	23	13	19	19	19	19
Cu	70	57	58	28	29	4	80	15	19	12	11
Zn	85	89	88	90	87	78	43	72	60	62	60
Pb	9	11	13	20	12	7	32	21	19	16	17
La	30	32	36	41	28	31	37	32	25	36	32
Ce	66	61	64	83	57	64	81	66	43	68	67
Th	7	7	5	11	6	7	10	9	7	10	9
Nd	29	27	28	37	26	32	32	30	20	28	28
U	3	3	1	3	2	2	2	2	4	3	1

*All Fe expressed as Fe^{2+} v, vitrophyre.

All analyses performed by the Geoanalytical laboratory at Washington State University.

Table 1—*Continued.*

Sample ID	KCS-16-27	KCS-16-21	KCS-16-38	KCS-16-20	KCS-16-49	KCS-16-22	KCS-16-35	KCS-16-36	KCS-16-51	KCS-16-39	KCS-16-29	KCS-16-30
Map unit	**Keld (v)**	**Keld**	**Keld**	**Keld**	**Keld (v)**	**Kemr**	**Kemr**	**Trt**	**Trt**	**Trt**	**Trt**	**Trt**
Lat	**46.39312**	**46.44069**	**46.42222**	**46.44532**	**46.44987**	**46.41986**	**46.43292**	**46.43222**	**46.44046**	**46.40495**	**46.41296**	**46.42103**
Long	**-112.39709**	**-112.44772**	**-112.43337**	**-112.43062**	**-112.40653**	**-112.40187**	**-112.44945**	**-112.44712**	**-112.47758**	**-112.42806**	**-112.41293**	**-112.41665**
XRF (wt. %)												
SiO_2	62.85	64.02	64.59	65.07	65.40	77.53	77.65	76.81	77.38	77.84	78.43	80.35
TiO_2	0.76	0.65	0.63	0.69	0.64	0.23	0.23	0.06	0.06	0.07	0.09	0.08
Al_2O_3	17.13	18.29	18.39	17.24	17.03	12.64	12.96	12.83	12.52	12.26	12.17	11.50
*FeO	5.01	3.47	3.19	3.90	3.66	0.58	0.98	1.17	1.26	1.31	1.39	1.33
MnO	0.10	0.07	0.06	0.10	0.10	0.03	0.03	0.03	0.02	0.01	0.01	0.01
MgO	1.96	1.31	0.95	1.47	1.26	0.16	0.22	0.07	0.01	0.00	0.14	0.02
CaO	5.39	5.01	4.64	4.53	4.40	0.54	0.34	0.31	0.16	0.21	0.31	0.14
Na_2O	3.14	3.40	3.46	3.07	4.00	3.53	6.54	4.01	3.87	3.53	2.63	2.10
K_2O	3.44	3.62	3.97	3.70	3.30	4.74	1.01	4.71	4.70	4.76	4.84	4.47
P_2O_5	0.22	0.15	0.13	0.23	0.22	0.01	0.02	0.01	0.02	0.00	0.01	0.00
LOI	0.88	1.86	4.35	3.86	1.07	0.50	0.87	0.86	0.76	1.04	1.89	1.71
a.t.	98.22	97.47	95.21	95.51	98.16	98.90	98.53	98.50	98.48	98.52	97.37	97.89
Trace elements (ppm) (XRF)												
Ni	4	11	4	13	5	12	6	3	4	3	3	3
Cr	20	19	5	32	6	66	17	5	3	3	5	4
Sc	13	10	9	11	10	4	4	1	1	0	1	1
V	102	64	49	68	68	8	13	5	2	0	5	4
Ba	1097	1282	1785	1253	1038	590	360	299	9	33	46	20
Rb	98	89	102	100	87	171	26	387	324	299	276	263
Sr	702	766	691	691	784	99	320	296	3	6	12	5
Zr	237	292	314	194	205	151	180	143	173	204	202	192
Y	25	24	22	24	25	28	27	66	89	39	43	37
Nb	11	11	11	11	11	17	16	93	84	75	71	67
Ga	18	19	18	18	18	13	11	31	31	29	28	28
Cu	14	9	5	8	4	4	4	1	1	4	2	2
Zn	69	50	46	63	54	14	20	131	132	136	108	94
Pb	18	20	20	17	23	21	25	55	48	44	37	38
La	35	36	34	33	36	45	44	10	19	14	30	26
Ce	71	66	66	67	66	82	75	36	56	21	77	44
Th	10	10	11	10	10	18	15	31	28	24	24	23
Nd	29	29	27	27	28	31	30	21	39	15	38	32
U	2	3	3	3	4	4	4	7	11	8	8	5

*All Fe expressed as Fe^{2+}

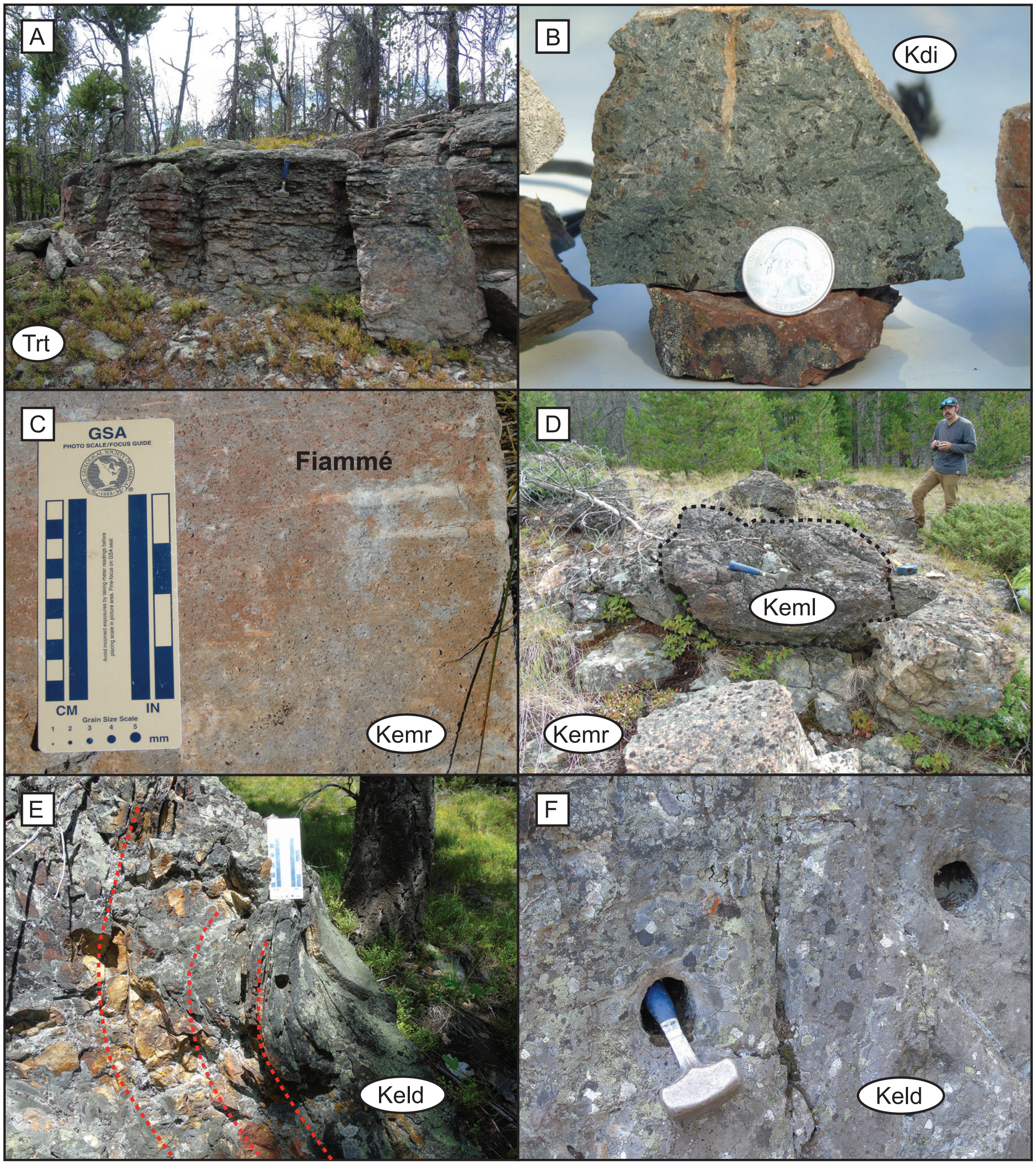

Figure 2. EMVF photographs. Rock compositions are shown on map figure 3. EMVF, Elkhorn Mountains Volcanic field. (A) Tertiary rhyolite ignimbrite (Trt). (B) Large hornblende crystals in diorite intrusion (Kdi). (C) Fiammé in rhyolite ignimbrite of the middle member EMVF (Kemr). (D) Block of basaltic andesite–andesite lava of the lower member EMVF (Keml) encased by rhyolite ignimbrite of the middle member EMVF (Kemr). (E) Ramp structure in dacite lavas of the lower member EMVF (Keld). (F) Voids in the lavas are interpreted to represent tree molds produced in the lava during lateral flow.

As much as 430 m of paleotopography channeled the movement of Tertiary silicic lavas and tuffs (Ruppel, 1963) between about 53 and 30 Ma (ages from Dudas and others, 2010; Mosolf, 2015). An extended period of erosion planed off the landscape, leaving isolated mountains that stood 150–300 m (492–984 ft) high (Ruppel, 1963). Middle Miocene basin and range block faulting (Reynolds, 1979) reactivated fault zones and revived stream incision in the Bison Mountain 7.5′ quadrangle. Pleistocene valley glaciers occupied the Little Blackfoot River, Ontario Creek, and many of their tributaries during the last glaciation. Valley glaciers were part of an ice sheet that attained a thickness of more than 300 m (984 ft) locally, and covered around 520 km^2 (201 mi^2) between Butte and Helena (Ruppel, 1962).

STRUCTURALGEOLOGY

The oldest rocks exposed are a gently folded, 200+ m (656+ ft) sequence of Paleozoic and Mesozoic sedimentary rocks that form the imbricated frontal edge of the 97 to 77 Ma Sapphire Thrust Plate (fig. 1) (Hyndman and others, 1975; Schmidt and others, 1994). The thrust plate formed concurrent with the Boulder Batholith–EMVF magma system. Fold-thrust belt deformation and batholith emplacement tilted Paleozoic–Mesozoic sedimentary and volcanic rocks about 5°–30° westward. The roof of the batholith is inclined about 10° to the northwest and forms sill-like lenses locally (Robertson, 1956).

Northeast-striking, high-angle, normal faults exhibit a component of right-lateral slip. These faults offset the contact between the Boulder Batholith and the EMVF by at least 1.6 km (5,249 ft) (Robertson, 1956). The Dog Creek Fault (see map) is a high-angle normal fault that has down to the southeast displacement of approximately130 m (426 ft) (Schmidt and others, 1994). The fault formed during a regional interval of magmatic inactivity between about 74 Ma and 53 Ma (Schmidt and others, 1994; ages from Olson and others, 2016; Dudas and others, 2010) and represents the southern boundary of the Sapphire Thrust Plate (fig. 1). The Monarch Fault Zone changes dip polarity along its strike (see map), is likely part of a broader shear zone, and exhibits about 160 m (525 ft) of down to the northwest net displacement. A 37 Ma rhyolite tuff (Trt) (figs. 3A, 3B) is banked into a footwall block in the fault zone north of the Monarch Mine (see map). These relationships suggest that the rhyolite tuff (Trt) accumulated in Tertiary extensional basins that formed prior to regional Miocene Basin and Range style block faulting (e.g., Reynolds, 1979). The rhyolite tuff (Trt) is offset by multiple small faults throughout the quadrangle, which is consistent with regional extension since about 37 Ma.

Northwest-trending lineaments are a conspicuous feature of the drainage pattern in the Bison Mountain 7.5' quadrangle, yet northwest-striking faults are observed only in underground mine workings where they are high-angle and display minor left-lateral displacement (Robertson, 1956). The quadrangle lies within a broad region of Quaternary seismicity characterized by north-striking block faults (Stickney and others, 2000) and NE–SW-directed extension (Stickney, 2015).

ECONOMIC GEOLOGY

The Elliston mining district overlaps the eastern half of the quadrangle (fig. 2 on map). Base metals occur in quartz lodes that occupy east-trending, high-angle fault systems (Robertson, 1956). Similar vein systems cut the Boulder Batholith–EMVF magma system throughout the region (Ruppel, 1963). Between 1894 and 1973, mines in the quadrangle produced nearly 15 million dollars (value in 2017) worth of Au, Ag, Cu, Pb, and Zn (table 2). Quartz veins are typically 1.5 m (5 ft) wide in the late Cretaceous granite (Kg) and transition to narrow stringers as they cut higher into EMVF rocks (Robertson, 1956). Exploration geologists mapped older mine workings in the Bison Mountain quadrangle as recently as the late 1980s (fig. 4).

Amygdaloidal zones (Keml) follow high-angle quartz veins and N30°W, 10°–20°SW-dipping autobrecciated flow margins in basaltic andesite–andesite lavas (Keml). Amygdaloidal lavas (fig. 4B on map) are associated with precious and base metal ore deposits in the Emery mining district, located about 8 km (5 mi) west of the quadrangle (fig. 1 on map). In the Emery district, Au, Ag, Pb, Zn, As, and Sb occur with sulfide minerals in calcite and quartz gangue (Robertson, 1953). Coarse andesitic breccia deposits (Kat) (fig. 4A on map) formed near a middle member EMVF vent, and are cut by mineral veins at Negro Mountain (Robertson, 1956).

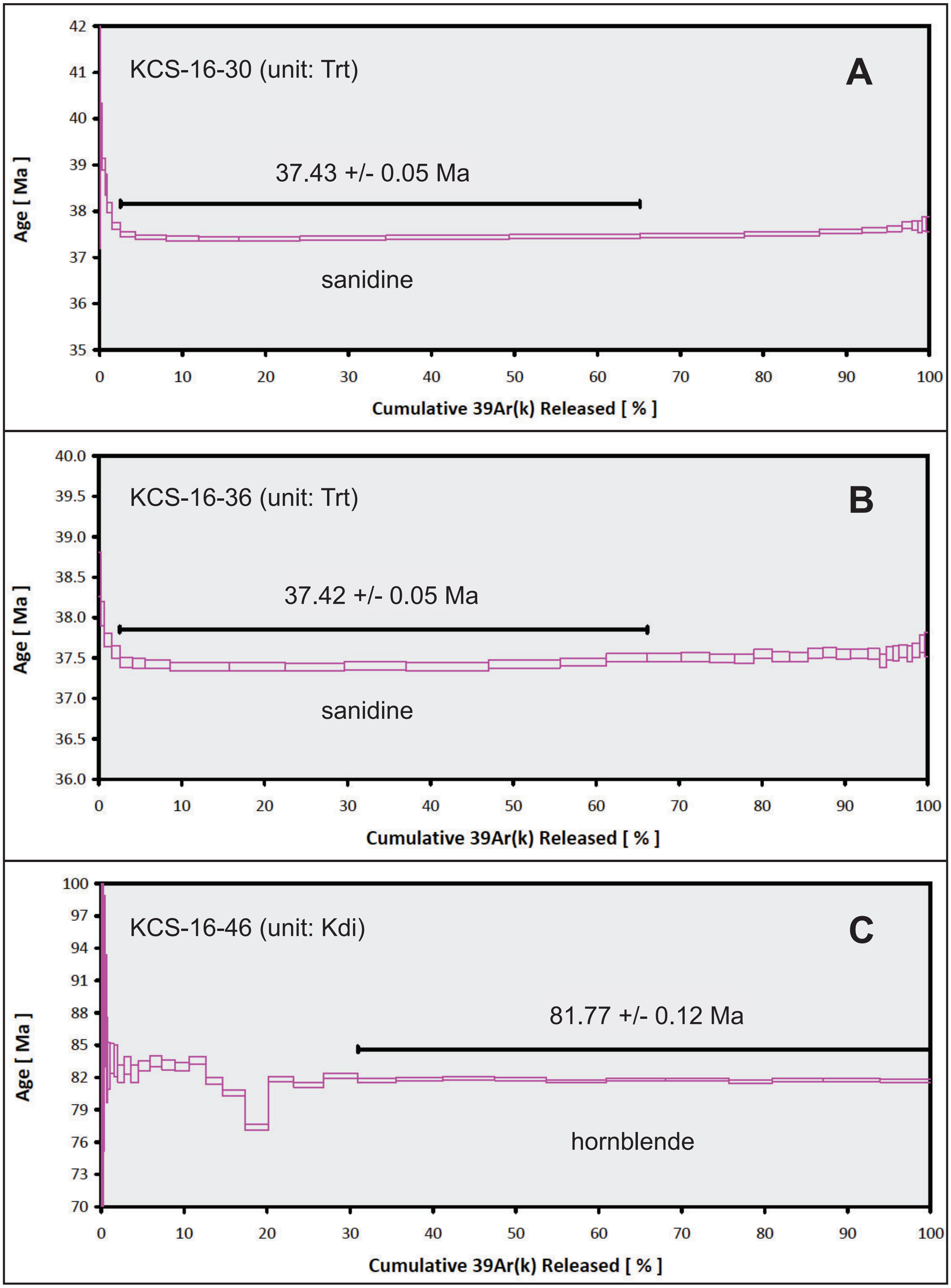

Figure 3. ^{40}Ar-^{39}Ar age spectra for samples collected in the Bison Mountain 7.5′ quadrangle. ^{39}Ar gas was extracted by bulk laser heating and analyzed over a series of incremental heating experiments using an ARGUS-VI-D at Oregon State University. The ages are thought to record the timing of volcanic eruptions.

Table 2. Historic mine production in the Bison Mountain 7.5′ quadrangle. Data compiled from Hargrave and others (1998) and references therein. Observations from this study (***bold/italics***).

Mine	Au (oz.)	Ag (oz.)	Cu (lbs.)	Pb (lbs.)	Zn (lbs.)	operating date	wall rock
Monarch (Mine and Mill)	157	10,677	25,034	96,514	48	1894-1909, 1916	***batholith (Kg) - EMVF (Kemr) contact***
Kimball Mine	-	-	-	-	-	-	andesitic volcanics ***(Kat)***
Treasure Mountain Mine	-	-	-	-	-	-	***batholith (kg) - EMVF (Kemr) contact***
Big Dick (Mill and Tailings)	7,687	51,236	1,870	716,553	3,800	1902-1954	porphyritic andesite breccia ***(Kat)***
Charter Oak (Mine and Mill)	382	39,146	10,041	672,046	168,270	1916-1966	Cretaceous andesite porphyry ***(Kat)***
Negros Mine	170	6,118	808	132,026	10,083	1946-1968	Cretaceous andesite porphyry ***(Kat)***
Golden Anchor	-	-	-	-	-	active in 1973	Cretaceous andesite porphyry ***(Kat)***
Totals	8,396	107,177	37,753	1,617,139	182,201	1894-1973	Kg-Kat contact, andesite volcanics
2017 market value ($'s/oz. or $'s/lb.)	1,281.90	18.23	2.55	0.99	1.17		
Total value (2017$'s)	10,762,832	1,953,837	96,270	1,600,968	213,175		
All commodities (2017$'s)	14,627,082						

Mine	vein orientation	vein width	vein mineralogy	alteration	gangue
Monarch (Mine and Mill)	***N80°E, 86° NW***	up to 6 m	a, c, g, p, s, t	a, c, l	q
Kimball Mine	N35°E, 48°-68° SE	50 cm	-	-	q
Treasure Mountain Mine	***N85°W, 78° SW***	-	-	-	-
Big Dick (Mill and Tailings)	E-W 20° N and N40°W and N50°E, 20° NW	-	a, bs, gc, p, s,	-	c, q
Charter Oak (Mine and Mill)	***NE 50°- 60°E***, 88° SE	15 - 90 cm	a, b, ga, s	pj	-
Negros Mine	NW-trending	-	p + q breccia	-	-
Golden Anchor	No conspicuous structure	-	-	-	
Totals	NE, E, NW, subvertical to 20° W, NW	15 cm to 6 m	a, b, bs, c, g, ga, gc, p, q, s, t	a, c, l, pj	c, q

Mineral abbreviations:
(a) = arsenopyrite, (b) = boulangerite, (bs) =black sphalerite, (c) = chalcopyrite, (g) = galena, (ga) = argentiferous galena, (gc) = galena w/chalcopyrite inclusions, (l) = limonite, (p) = pyrite, (pj) = plumbojarosite, (q)= quartz, (s) = sphalerite, (t) = tetrahedrite.

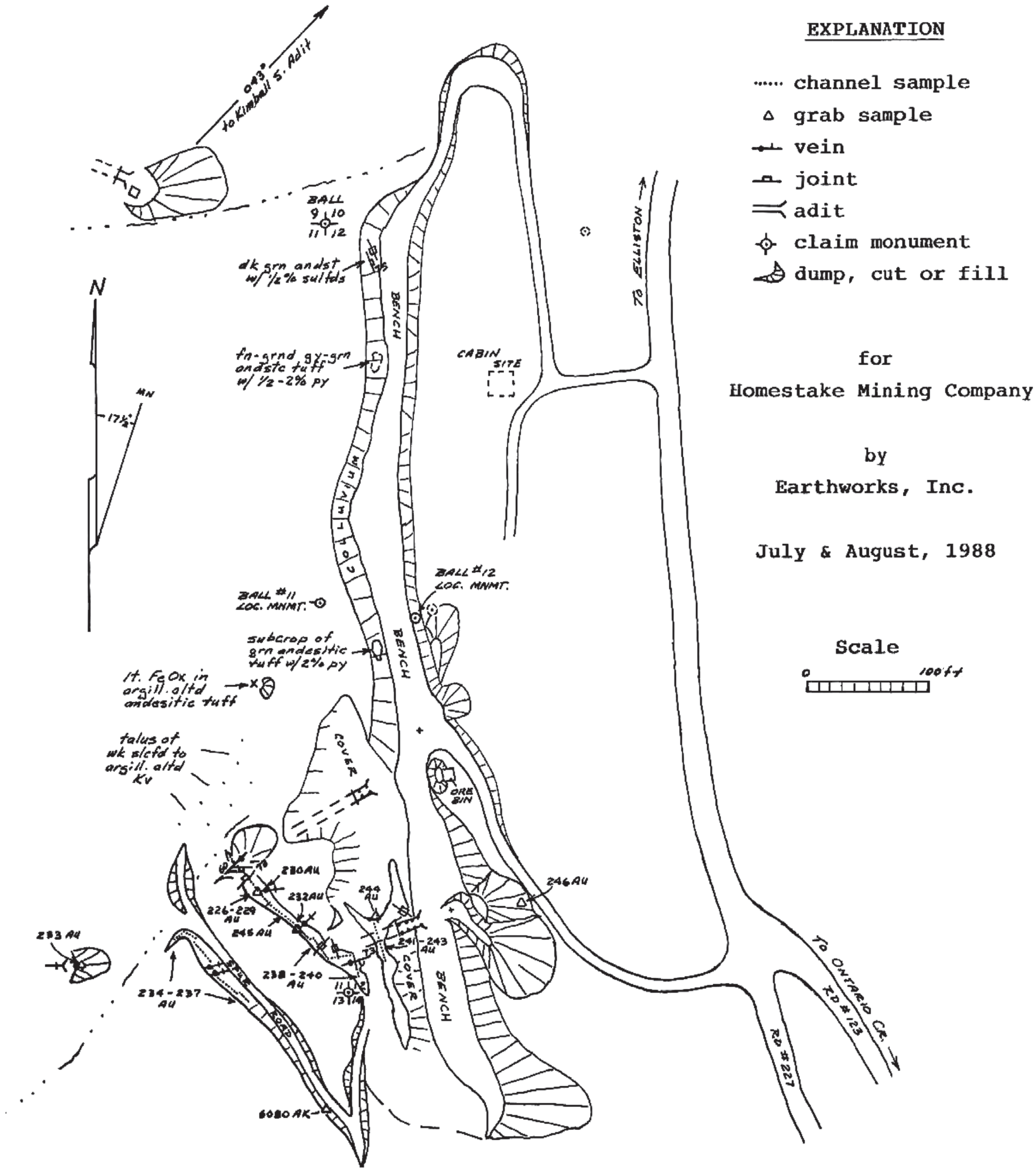

Figure 4. Map of the Kimball Mine workings northwest of the junction of Ontario Creek with the Little Blackfoot River. Mapped by Bruce Cox, Earthworks, Inc.

REFERENCES CITED

Berg, R.B., and Hargrave, P.A., 2004, Geologic map of the Upper Clark Fork Valley: Montana Bureau of Mines and Geology Open-File Report 506, scale 1:50,000.

Dudas, F.O., Ispolatov, V.O., Harlan, S.S., and Snee, L.W., 2010, $^{40}Ar/^{39}Ar$ geochronology and geochemical reconnaissance of the Eocene Lowland Creek volcanic field, west-central Montana: Journal of Geology, v. 118, no. 3, p. 295–304.

Hargrave, P.A., Bowler, T.P., Lonn, J.D., Madison, J.P., Metesh, J.J., and Wintergerst, R., 1998, Abandoned–inactive mines of the Blackfoot and Little Blackfoot River drainages, Helena National Forest Volume II: Montana Bureau of Mines and Geology Open-File Report 368, 159 p.

Hyndman, D.W., Talbot, J.L., and Chase, R.B., 1975, Boulder Batholith: A result of emplacement of a block detached from the Idaho Batholith infrastructure?: Geology, v. 3, p. 401–404.

Klepper, M.R., Weeks, R.A, and Ruppel, E.T., 1957, Geology of the southern Elkhorn Mountains, Jefferson, and Broadwater Counties, Montana: U.S. Geological Survey Professional Paper 292, 82 p.

Klepper, M.R., Ruppel, E.T., Freeman, V.L., and Weeks, R.A., 1971, Geology and mineral deposits, east flank of the Elkhorn Mountains, Broadwater County, Montana: U.S. Geological Survey Professional Paper 665, scale 1:48,000.

Korzeb, S.L., Scarberry, K.C., and Zimmerman, J.L., 2018, Interpretations and genesis of Cretaceous age veins and exploration potential for the Emery Mining District, Powell County, Montana: Montana Bureau of Mines and Geology Bulletin 137, 60 p., 1 sheet, scale 1:24,000.

Lageson, D., Schmitt, J., Horton, B., Kalakay, T., and Burton, B., 2001, Influence of Late Cretaceous magmatism on the Sevier orogenic wedge, western Montana: Geology, v. 29, p. 723–726.

Le Bas, M.J., LeMaitre, R.W., Streckeisen, A., and Zanettin, B., 1986, A chemical classification of volcanic rocks based on the total alkali silica diagram: Journal of Petrology, v. 27, p. 745–750.

Lewis, R.S., 1998, Geologic map of the Butte 1º x 2º quadrangle, southwestern Montana: Montana Bureau of Mines and Geology Open-File Report 363, 16 p., 1 sheet, scale 1:250,000.

Lund, K., Aleinikoff, J., Kunk, M., Unruh, D., Zeihen, G., Hodges, W., duBray, E., and O'Neill, J., 2002, SHRIMP U-Pb and $^{40}Ar/^{39}Ar$ age contrasts for relating plutonism and mineralization in the Boulder batholith region, Montana: Economic Geology, v. 97, p. 241–267.

Martin, M., and Dilles, J., 2000, Timing and duration of the Butte porphyry system: Northwest Geology, v. 25, p. 1.

Mosolf, J.G., 2015, Geologic field guide to the Tertiary volcanic rocks in the Elliston 30' x 60' quadrangle, west-central Montana: Northwest Geology, v. 44, p. 213–232.

Olson, N.H., Dilles, J.H., Kallio, I.M., Horton, T.R., and Scarberry, K.C., 2016, Geologic map of the Ratio Mountain 7.5′ quadrangle, southwest Montana: Montana Bureau of Mines and Geology EDMAP-10, scale 1:24,000.

Prostka, H.J., 1966, Igneous geology of the Dry Mountain quadrangle, Jefferson County, Montana: U.S. Geological Survey Bulletin 1221-F, scale 1:24,000.

Reynolds, M.W., 1979, Character and extent of Basin-Range faulting, western Montana and east-central Idaho, *in* Newman, G.W., and Goode, H.D., eds.: Rocky Mountain Association of Geologists and Utah Geological Association Basin and Range Symposium, p. 185–193.

Robertson, F.R., 1953, Geology and mineral deposits of the Zosell (Emery) mining district, Powell County, Montana: Montana Bureau of Mines and Geology Memoir 34, 29 p., 6 plates.

Robertson, F.R., 1956, Geology and mineral deposits of the Elliston mining district, Powell County, Montana: Seattle, University of Washington, Ph.D. dissertation, 332 p.

Ruppel, E.T., 1962, A Pleistocene ice sheet in the northern Boulder Mountains, Jefferson, Powell, and Lewis and Clark Counties, Montana: U.S. Geological Survey Bulletin 1141-G, 22 p.

Ruppel, E.T., 1963, Geology of the Basin quadrangle, Jefferson, Lewis and Clark, and Powell Counties, Montana, U.S. Geological Survey Bulletin 1151, 121 p., scale 1:62,500.

Rutland, C., Smedes, H., Tilling, R., and Greenwood, W., 1989, Volcanism and plutonism at shallow crustal levels: The Elkhorn Mountains Volcanics and the Boulder Batholith, southwestern Montana, *in* Henshaw, P., ed.: Volcanism and plutonism of western North America; Volume 2, Cordilleran volcanism, plutonism, and magma generation at various crustal levels, Montana and Idaho, Field trips for the 28th International Geological Congress: American Geophysical Union Monograph, p. 16–31.

Scarberry, K.C., 2016, Geologic map of the Wilson Park 7.5′ quadrangle, southwestern Montana: Montana Bureau of Mines and Geology Geologic Map 66, scale 1:24,000.

Scarberry, K.C., Kallio, I.M., Olson, N., Dilles, J.H., Older, C.W., Horton, T., and English, A.R., 2016, Large-volume pyroclastic deposits along the eastern edge of the Boulder Batholith, southwestern Montana: Geological Society of America Abstracts with Programs, v. 48, no. 4.

Scarberry, K.C., Kallio, I.M., and English, A.R., 2017, Geologic map of the Boulder East 7.5′ quadrangle, southwestern Montana: Montana Bureau of Mines and Geology Geologic Map 68, scale 1:24,000.

Schmidt, R.G., Loen, J.S., Wallace, C.A., and Mehnert, H.H., 1994, Geology of the Elliston region, Powell and Lewis and Clark Counties, Montana: U.S. Geological Survey Bulletin 2045, 25 p., scale 1:62,500.

Sears, J.W., 2016, Belt-Purcell Basin: Template for the Cordilleran magmatic arc and its detached carapace, Idaho and Montana, *in* MacLean, J.S., and Sears, J.W., eds:, Belt Basin: Window to Mesoproterozoic earth: Geological Society of America Special Paper 522, p. 365–384.

Smedes, H.W., 1962, Lowland Creek volcanics, an Upper Oligocene formation near Butte, Montana: The Journal of Geology, v. 70, no. 2.

Smedes, H.W., 1966, Geology and igneous petrology of the northern Elkhorn Mountains, Jefferson and Broadwater Counties, Montana: U.S. Geological Survey Professional Paper 510, 82 p., 1:48,000 scale map.

Smedes, H.W., and Thomas, H.H., 1965, Reassignment of the Lowland Creek volcanics to Eocene age: Journal of Geology, v. 73, no. 3, p. 508–510.

Stickney, M.C., Haller, K.M., and Machette, M.N., 2000, Quaternary faults and seismicity in western Montana: Montana Bureau of Mines and Geology Special Publication 114, 1 sheet, scale 1:750,000.

Stickney, M.C., 2015, Seismicity within and adjacent to the eastern Lewis and Clark Line, west-central Montana: Northwest Geology, v. 44, p. 19–35.

Vuke, S.M., Porter, K.W., Lonn, J.D., and Lopez, D.A., 2007, Geologic map of Montana: Montana Bureau of Mines and Geology Map 62A, scale 1:500,000.

Wallace, C.A., Lidke, D.J., and Schmidt, R.G., 1990, Faults of the central part of the Lewis and Clark line and fragmentation of the Late Cretaceous foreland basin in west-central Montana: Geological Society of America Bulletin, v. 102, p. 1021–1037.